Probing the Structures of Neutral Boron Clusters Using IR/VUV Two Color Ionization: B_{11}, B_{16}, and B_{17}

Constantin Romanescu,[1] Dan J. Harding,[2] André Fielicke,[2,a)] and Lai-Sheng Wang[1,b)]

[1]Department of Chemistry, Brown University, Providence, RI 02912, USA

[2]Fritz-Haber-Institut der Max-Planck-Gesellschaft, Faradayweg 4-6, D-14195 Berlin, Germany

[a)] Electronic mail: fielicke@fhi-berlin.mpg.de

[b)] Electronic mail: Lai-Sheng_Wang@brown.edu

Abstract

The structures of neutral boron clusters, B_{11}, B_{16}, and B_{17}, have been investigated using vibrational spectroscopy and *ab initio* calculations. Infrared absorption spectra in the wavelength range of 650 to 1550 cm^{-1} are obtained for the three neutral boron clusters from the enhancement of their near-threshold ionization efficiency at a fixed UV wavelength of 157 nm (7.87 eV) after resonant absorption of the tunable infrared photons. All three clusters, B_{11}, B_{16}, and B_{17}, are found to possess planar or quasi-planar structures, similar to their corresponding anionic counterparts (B_n^-), whose global minima were found previously to be planar using photoelectron spectroscopy and theoretical calculations. Only minor structural changes are observed between the neutral and the anionic species for these three boron clusters.

I. INTRODUCTION

Boron is an electron-deficient element with four valence orbitals and only three valence electrons. As a consequence, bulk boron features three-dimensional (3D) structures based on cage-like structural units (B_{12} icosahedron, B_6 octahedron, or B_{12} cuboctahedron), with extensive electron sharing.[1,2] Early experimental works on boron clusters in the late 1980s attributed similar 3D structures to the cationic boron clusters observed in mass spectrometric investigations, including the highly stable B_{13}^+ cluster.[3] Computational investigations suggested, however, that for isolated boron clusters the cage-like structures were unstable and that planar or quasi-planar structures were energetically favored.[4-9] Over the past decade, photoelectron spectroscopy (PES) of size-selected clusters on negatively charged boron cluster (B_n^-) in conjunction with ab initio calculations has revealed that boron cluster anions are planar or quasi-planar up to at least $n = 21$.[10-20] Although the 2D-to-3D transition for anionic clusters is not known, that for neutral clusters[15] was suggested to occur at B_{20} and for cationic clusters[21] at B_{16}^+. The first 3D structure for B_{20} was found to have a double-ring shape (C_{5v})[15] and the transition size for the neutral clusters at B_{20} has been reproduced by recent calculations.[22] All planar boron clusters have been found to consist of a peripheral boron ring, which is characterized by strong classical two-center two-electron (2c-2e) covalent bonds, and one or more inner boron atoms bonded to the peripheral boron ring by delocalized σ and π bonds.[10-20,23] The latter gives rise to the concept of multiple aromaticity and antiaromaticity, depending on the electron count of the delocalized bonds. For larger clusters, it is anticipated that localized covalent bonds may contribute also to the bonding of the inner atoms, as observed recently in the planar B_{21}^- cluster.[20]

While the structures and bonding models established for the anionic boron clusters are expected to be valid for the neutral clusters, no direct experimental studies on neutral boron clusters have been done, except for B_3.[24,25] In addition, the disagreement between cluster structures, which were calculated using different computational methods, as demonstrated recently for B_{14},[22,26] calls for an experimental investigation of the structures of neutral boron clusters. Photoelectron spectroscopy studies of size-selected anions often provide spectroscopic information about the corresponding neutrals. However, if the global minimum of the neutral is different from that of the anion, photodetachment may not access the global minimum of the neutral state because photodetachment is essentially a vertical process.

In the current article, we report a vibrational spectroscopy study of neutral boron clusters using tunable IR + fixed UV two color ionization (IR-UV2CI). In IR-UV2CI, one uses UV photons (157 nm in the current case) to ionize the neutral clusters near the ionization threshold. Heating of the clusters via resonant absorption of the IR photons can lead to an enhancement in the ionization efficiency for a given cluster if its ionization potential (IP) is just above the UV photon energy. Recording this enhancement as a function of the IR excitation wavelength provides size-specific IR spectra for neutral clusters. This technique was first used to obtain IR spectra of jet-cooled molecules,[27] clusters,[28] and an Al-organic complex.[29] It has been successfully applied to the study of neutral silicon[30,31] and magnesium oxide[32] clusters recently. Comparison of the IR absorption spectra with results from *ab initio* calculations allows neutral structural information to be obtained. In the present study, we have obtained IR spectra in the wavelength range from 650 to 1550 cm^{-1} for three neutral boron clusters B_n (n = 11, 16, 17) using the IR-UV2CI method. Theoretical calculations using density functional theory (DFT) have been carried out and compared with the experimental data. The joint experimental and

computational study shows that all three neutral boron clusters are planar, similar to the global minimum of the corresponding anions.

II. EXPERIMENTAL AND THEORETICAL METHODS

An essential step in the IR-UV2CI experiment for the neutral boron clusters was their ionization. Since there were no prior reports of experimental measurements of the IPs of neutral boron clusters, we calculated the IPs and the IR spectra of boron clusters using DFT methods, based on the low-energy isomers reported in the literature. This information was important for us to assess the feasibility of the IR-UV2CI experiment, because of the availability of our UV and IR sources. We found that B_n clusters with $n \geq 10$ have calculated IPs spanning approximately the range of ~7–9 eV and they have strong IR active modes in the wavelength range between 700–1500 cm^{-1}, suggesting that at least for some B_n clusters the IR-UV2CI experiment should be feasible using a fixed UV source at 157 nm (7.87 eV) from an F_2 excimer laser and the FELIX IR source, which is tunable between 3–250 μm. The calculated IPs are given as Supplementary Material (Fig. S1).[33]

A. Experimental details

The experiment was carried out using a molecular beam apparatus equipped with a laser vaporization source and a reflectron time-of-flight mass spectrometer (TOF-MS), details of which have been described elsewhere.[34] Briefly, boron clusters were produced by laser vaporization of an isotopically enriched ^{11}B rod (99.4%) and equilibrated in a thermalization channel cooled to 140 K using liquid nitrogen. The cluster beam was collimated first by a skimmer and then passed a 1 mm diameter flat aperture, which was used to remove the charged clusters from the beam by an applied DC voltage. The neutral clusters were ionized in the extraction region of the TOF-MS by 157 nm (7.87 eV) photons from a pulsed F_2 excimer laser.

Neutral clusters that have IPs lower than 7.87 eV could be efficiently ionized, even though residual signals were detected for species with slightly higher computed IPs (Fig. 1, upper trace). For the latter, the residual signals were probably due to ionization of "hot' clusters. IR absorption spectra were obtained by overlapping the cluster beam with a counter-propagating IR beam from the Free Electron Laser for Infrared eXperiments (FELIX). The IR laser delivered ~5 μs long pulses, with energies of 20-40 mJ/pulse and a bandwidth of 0.5 % of the central wavelength. The IR beam was loosely focused ~30 mm behind the 1 mm diameter flat aperture. Upon resonant absorption of IR photons, the internal energy of the cold clusters was raised, resulting in an increased ionization efficiency (see lower trace in Fig. 1). The cluster size-specific IR spectra were obtained by recording mass spectra on alternating shots with the FELIX radiation ON (intensity I) and OFF (intensity I_0). Relative absorption spectra were derived from the enhancements of the ion signals by $(I - I_0)/I_0$ normalized by the IR beam energy, as a function of the IR wavelength scanned from 650–1450 cm^{-1}. Because the UV ionization laser was fixed and the clusters were expected to have size-dependent IPs, we expected that only those neutral clusters with IPs slightly above the UV photon energy to exhibit an enhancement in their ionization efficiency upon IR absorption. Hence, although the mass signals were recorded for a large size range simultaneously, as shown in Fig. 1, good IR absorption spectra were obtained only for B_{11}, B_{16}, and B_{17}.

B. Theoretical calculations

To obtain cluster structure information, comparison with calculated IR spectra was required. Based on previous experiences with *ab initio* calculations for anionic boron clusters, structure optimization and IR spectra calculations at DFT level were carried out for comparison with the observed vibrational spectra. One problem that had been recognized by a number of

groups previously was that some density functionals, such as B3LYP,[35-37] performed poorly when calculating the relative energies of the B_n isomers, especially when comparing isomers with 2D and 3D structures.[38,39] However, we found that the optimized structures and the calculated vibrational spectra did not differ significantly using different functionals. The calculations reported in this study were done with the B3LYP, PBE0,[40] and TPSS[41] functionals and the 6-311+G(d) basis set[42-44] using the Gaussian03 program suite.[45] For B_{11} and B_{16}, we generated roughly 300 random structures each, which were first optimized at the PBE0/3-21G[46] levels of theory. The low-energy isomers at the PBE0/3-21G level of theory were reoptimized with a larger basis set of 6-311+G(d). For both clusters, we identified the putative global minimum structures reported in previous theoretical studies along with other low-lying isomers. For B_{17}, as a starting point, we used the structures that were previously reported for B_{17}^-,[19] B_{17},[22] and B_{17}^+.[21] The IR frequencies calculated at the B3LYP/6-311+G(d) level of theory were rescaled with a multiplication factor of 0.96, which was found to be in good agreement with the literature value for the same level of theory, i.e., 0.968.[47] For the other two functionals, we found that multiplication factors of 0.95 (PBE0) and 0.975 (TPSS) gave the best agreement with experiment.

III. RESULTS AND DISSCUSSION

Our initial goal was to investigate the structures of neutral boron clusters (B_n) with $n \geq 10$. However, at the 7.87 eV ionization energy, we found that only three clusters gave vibrational spectra with good signal-to-noise ratios: B_{11}, B_{16}, and B_{17}, as shown in the top trace of Figs. 2-4, respectively. For the remaining clusters, for which good IR spectra were not obtained, there were two possibilities, their IPs are either lower than 7.87 eV or too high above

7.87 eV. The IPs calculated (Fig. S1)[33] provide some rationales for our experimental observations. The IPs of B_{13}, B_{15}, B_{19}, and B_n for $n \geq 21$ appear to be below 7.87 eV and were observed to be ionized efficiently by a single photon at 7.87 eV, as shown in the upper trace of Fig. 1. Consequently, we observed no IR-induced enhancement for these clusters. The remaining clusters, B_{10}, B_{12}, B_{14}, B_{18}, and B_{20}, showed very weak IR-induced enhancement, which did not yield useful IR spectra for these clusters in the FELIX wavelength range between 650 and 1550 cm^{-1}. The calculated IPs (Fig. S1)[33] showed indeed that the IPs of these clusters are significantly higher than 7.87 eV, except B_{20}. Consequently, these clusters could not be excited high enough via IR pumping to be ionized efficiently with the 157 nm UV laser. A notable exception was B_{20}, for which the calculated lowest-energy isomer was the C_{5v} double ring. Its IP was calculated to be 7.46 eV, clearly below the 157 nm photon energy, but the mass spectrum (Fig. 1) showed only a weak signal. This suggested that either the IP calculation was not accurate enough or the global minimum of neutral B_{20} has not been identified. A similar situation was reported for the corresponding anion B_{20}^-, whose global minimum was also computed to be the double ring, but it was not present in the photoelectron spectra.[15]

The calculated IR spectra of the global minimum and three low-lying isomers in the wavelength range of 650 to 1550 cm^{-1} for B_{11}, B_{16}, and B_{17} are compared with the experimental data in Figs. 2-4, respectively. The corresponding structures with the relative energies calculated at different levels of theory for the three clusters are shown in Fig. 5. Even though the relative energies vary slightly, all three levels of theory gave rise to the same global minimum structure, which in each case yielded the best agreement with the experimental data. To simplify the following discussion, the relative energies of the B_n isomers will refer to the PBE0/6-311G+(d) calculations, which were found to agree well with higher level coupled-clusters calculations.[37]

A. B_{11}. The IR spectrum of B_{11} (Fig. 2) shows a strong band at around 915 cm^{-1} with a number of weak peaks in the wavelength range from 650 to 1550 cm^{-1}. Recent theoretical calculations suggested that in the ground electronic state B_{11} has a C_{2v} symmetry and a $^2B_2$ electronic state (11.I, Fig. 5A).[48] It consists of a boron dimer located inside a nine-membered boron ring, similar to the ground state of B_{11}^-.[13] An alternative low-lying C_{2v} isomer[48] was found to be a first order saddle point on the potential energy surface and further optimization along the imaginary frequency coordinate led to the ground state isomer. All other identified isomers of B_{11} lie relatively high in energy compared to 11.I, as shown in Fig. 5. The next isomer, 11.II (C_s, $^2A'$, +0.73 eV), also reported for B_{11}^-, features a three-membered ring inside an eight-membered ring. The next two isomers, 11.III (C_s, $^2A'$) and 11.IV (C_{2h}, ^2A_g), lie even higher in energy, at 1.14 eV and 2.16 eV, respectively. Given the large energy difference between 11.I and 11.II (0.73 eV), it might be expected that only the lowest energy isomer would be present in the cluster beam. Indeed, the calculated IR spectrum of 11.I shows a good agreement with the measured IR spectrum (Fig. 2), confirming firmly the identified global minimum for B_{11}.

The previous study on B_{11}^- using photoelectron spectroscopy and theoretical calculation found that there was a small geometry change between the ground state of the anion and that of its neutral.[13] The photoelectron spectrum resolved two vibrational modes for the ground state transition with frequencies of 1040 ± 50 cm^{-1} and 480 ± 40 cm^{-1}, which were assigned to the symmetric stretching of the B-B bond connecting the inner atoms (1092 cm^{-1}) and the symmetric stretching of the peripheral atoms relative to the inner atoms (481 cm^{-1}), respectively. These symmetric modes are not IR-active. It should be pointed out that B_{11}^+ is quasi-planar with a B_2 unit inside a B_9 ring (C_s, $^1A'$),[6] but the B_2 unit is slightly out of the B_9 plane.

Chemical bonding analyses provide further insights into the similarities and differences between the equilibrium geometries of B_{11} at different charge states. B_{11}^- constitutes a prototypical system for the investigation of the concepts of aromaticity/antiaromaticity and the analogy between boron clusters and hydrocarbons.[13,16] Detailed bonding analyses of B_{11}^- showed that its 34 valence electrons form nine 2c-2e peripheral σ-bonds (18 e^-), three 11c-2e delocalized π-bonds (6 e^-), and five 3c-2e delocalized σ-bonds (10 e^-). The delocalized σ and π systems, which each conform to the $4N$+2 Hückel rule for aromaticity, make B_{11}^- doubly aromatic (6 π electrons and 10 σ electrons). The B_{11}^- cluster was regarded as the all-boron analogue of $C_5H_5^-$ according to their similar π bonding.[13] The highest occupied molecular orbital (HOMO) of B_{11}^- belong to the σ-delocalized MOs, and, therefore, B_{11} retains the π-aromaticity of B_{11}^- upon one electron removal from its HOMO. The overall effect from B_{11}^- to B_{11} is the weakening of the delocalized σ-bonding between the inner atoms and the peripheral atoms, which results in a shorter inner B-B distance in B_{11} compared to B_{11}^- (1.72 Å vs. 1.77 Å), while the perimeter of the outer B_9 ring does not change. Further removal of the unpaired electron from B_{11} results in a system that exhibits conflicting π-aromaticity and σ-antiaromaticity (only 8 σ-delocalized electrons) in B_{11}^+. As a result, B_{11}^+ has a quasi-planar geometry with the two inner atoms distorted slightly above and below the B_9 plane, respectively.

B. B_{16}. The experimental IR spectrum of B_{16} is compared with the computed spectra of the low-lying isomers in Fig. 3. Two strong IR bands were observed in the wavelength range of 650 to 1550 cm^{-1} at around 850 cm^{-1} and 1120 cm^{-1}. Previous photoelectron spectroscopy and theoretical studies found that B_{16}^- has a quasi-planar structure,[17] while ion mobility studies revealed that B_{16}^+ prefers 3D structures,[21] marking the onset of 2D–3D transition for boron cluster cations. The lowest energy structure found in the current work for B_{16} is isomer 16.I (C_{2h},

^1A_g) in Fig. 5B, which is similar as that identified for B_{16}^- in the previous combined photoelectron spectroscopy and theoretical study,[17] as well as a recent calculation.[22] A 3D structure with a geometry similar to that of B_{16}^+ is found to be the second isomer, 16.II (C_{2v}, $^1A_1$) in Fig. 5B, at the PBE0 level. Its energy is close to that of two other 2D isomers, 16.III (C_s, $^1A'$) and 16.IV (C_1, ^1A). The excellent agreement between the experimental IR spectrum and the calculated spectrum for 16-I confirms unequivocally that isomer 16.I is the global minimum for the neutral B_{16} cluster.

The chemical bonding of B_{16} is similar to that of B_{16}^- and B_{16}^{2-}.[17] The 48 valence electrons of B_{16} participate in the formation of 12 peripheral B–B σ-bonds, 8 delocalized (*n*c-2e) σ-bonds responsible for bonding the 4 inner B atoms to the peripheral ring, and 4 delocalized π-bonds. This bonding situation makes the B_{16} cluster doubly antiaromatic, which results in its elongated shape and quasi-planar geometry. As a comparison, the B_{16}^{2-} cluster is π-aromatic and σ-antiaromatic and has a perfect planar structure with C_{2h} symmetry.

C. B_{17}. The experimental IR spectrum of B_{17} is compared with the computed spectra of the low-lying isomers in Figure 4. The B_{17} spectrum is more complicated and has relatively poor signal-to-noise ratios. Four IR bands can be identified: a broad band around 860 cm^{-1}, and three relatively sharper bands at 1150 cm^{-1}, 1260 cm^{-1}, and 1450 cm^{-1}. The calculated structures of the corresponding isomers are shown in Fig. 5C. Similar to the case of B_{16}, previous experimental works on the charged clusters demonstrated that the most stable structure of B_{17}^- has a perfect planar geometry,[19] while that of B_{17}^+ prefers the 3D structure.[21] We have investigated a range of structures for B_{17}, including those reported for B_{17}^- and B_{17}^+ and those reported in a recent theoretical work.[22] The planar B_{17}^- (C_{2v}, $^1A_1$) consists of a 12-membered peripheral ring and 5 inner boron atoms, similar to that of structure 17.II (C_{2v}, $^2A_2$) (Fig. 5C).[19] This structure does not

give a good agreement with the experimentally measured IR spectrum. Moreover, we found that at the TPSS/ 6-311+G(d) level of theory the 17.II structure has one imaginary frequency. Further optimization along the normal coordinate corresponding to the imaginary frequency lead to a lower symmetry, lower energy structure, 17.I (C_1, ^2A) as shown in Fig. 5C, that was recently reported as the global minimum for B_{17}.[21] As a matter of fact, isomer 17.I and structure 17.II are very similar with only a slightly different location for one of the five inner B atoms. This geometry change between the anionic and neutral cluster is consistent with the broad photoelectron spectra observed for B_{17}^-.[19] Thus, the excellent agreement between the experimental and the calculated IR spectra confirm that isomer 17.I is the global minimum for B_{17}.

The higher energy isomers are the quasi-planar 17.III (C_s, $^2A'$) and the 3D 17.IV (C_s, $^2A'$) structures, also reported in a recent theoretical report.[22] The bonding analysis performed for the ground state B_{17}^- (C_{2v}, $^1A_1$) has shown that the system is doubly aromatic with 18 delocalized σ electrons and 10 delocalized π electrons. The remaining 24 electrons participate in twelve 2c-2e B-B bonds for the peripheral 12-membered boron ring.[19] In most of the larger boron clusters ($n \geq 10$), the inner boron atoms are not connected by classical 2c-2e bonds. Instead they are bound to the peripheral atoms via delocalized σ-radial bonds, and the internuclear distances between the inner atoms are usually longer than the peripheral B–B σ-bonds (~1.6 Å). Detachment of a single electron from the HOMO of B_{17}^- (*n*c-2e σ-bond) weakens the interaction between the inner boron atoms and the peripheral ring and shortens the distance between the inner atoms, similar to the situation encountered for the B_{11} cluster. This effect led to the occurrence of pentagonal and hexagonal holes in larger quasi-planar boron clusters.[20,49,50] This electron

deficiency should also be the reason why stable bulk 2D sheets have been shown to contain regular hexagonal holes.[51]

IV. CONCLUSIONS

We have investigated the structural properties of three neutral boron clusters using a joint IR vibrational spectroscopy and *ab initio* computational study. We find that planar structures are favored for all three cluster sizes, consistent with previous experimental work on negatively charged boron clusters and predictions made by theory for the neutral clusters. We showed that vibrational spectra can be obtained for neutral boron clusters using the IR/UV two-color ionization scheme. With a tunable UV source, this two-color ionization scheme should be able to allow vibrational spectra of all small to medium-sized neutral boron clusters to be investigated.

ACKNOWLEDGEMENTS

This work was supported by U.S. National Science Foundation (DMR-0904034 to L.S.W.) and by the Deutsche Forschungsgemeinschaft within FOR 1282 (FI 893/4-1 to A. F.). The authors gratefully acknowledge the support of the Stichting voor Fundamenteel Onderzoek der Materie (FOM) in providing beam time on FELIX and highly appreciate the skillful assistance of the FELIX staff. D.J.H. thanks the Alexander von Humboldt Foundation for a fellowship.

REFERENCES

1. F. A. Cotton, G. Wilkinson, C. A. Murillo, and M. Bochmann, *Advanced Inorganic Chemistry*, 6 ed. (Wiley-Interscience, New York, 1999).
2. N. N. Greenwood and A. Earnshaw, *Chemistry of the Elements*. (Butterworth-Heinemann Limited, 1997).
3. L. Hanley, J. L. Whitten, and S. L. Anderson, J. Phys. Chem. **92**, 5803 (1988).
4. R. Kawai and J. H. Weare, J. Chem. Phys. **95**, 1151 (1991).
5. H. Kato, K. Yamashita and K. Morokuma, Chem. Phys. Lett. **190**, 361 (1992).
6. I. Boustani, Int. J. Quant. Chem. **52**, 1081 (1994).
7. I. Boustani, Chem. Phys. Lett. **233**, 273 (1995).
8. A. Ricca and C. W. Bauschlicher, Chem. Phys. **208**, 233 (1996).
9. I. Boustani, Phys. Rev. B **55**, 16426 (1997).
10. H. J. Zhai, L. S. Wang, A. N. Alexandrova, and A. I. Boldyrev, J. Chem. Phys. **117**, 7917 (2002).
11. A. N. Alexandrova, A. I. Boldyrev, H. J. Zhai, L. S. Wang, E. Steiner, and P. W. Fowler, J. Phys. Chem. A **107**, 1359 (2003).
12. H. J. Zhai, A. N. Alexandrova, K. A. Birch, A. I. Boldyrev, and L. S. Wang, Angew. Chem. Int. Ed. **42**, 6004 (2003).
13. H. J. Zhai, B. Kiran, J. Li, and L. S. Wang, Nature Mat. **2**, 827 (2003).
14. A. N. Alexandrova, A. I. Boldyrev, H. J. Zhai, and L. S. Wang, J. Phys. Chem. A **108**, 3509 (2004).
15. B. Kiran, S. Bulusu, H. J. Zhai, S. Yoo, X. C. Zeng, and L. S. Wang, Proc. Nat. Acad. Sci. USA **102**, 961 (2005).
16. A. N. Alexandrova, A. I. Boldyrev, H. J. Zhai, and L. S. Wang, Coord. Chem. Rev. **250**, 2811 (2006).
17. A. P. Sergeeva, D. Y. Zubarev, H. J. Zhai, A. I. Boldyrev, and L. S. Wang, J. Am. Chem. Soc. **130**, 7244 (2008).
18. W. Huang, A. P. Sergeeva, H. J. Zhai, B. B. Averkiev, L. S. Wang, and A. I. Boldyrev, Nature Chem. **2**, 202 (2010).

19. A. P. Sergeeva, B. B. Averkiev, H. J. Zhai, A. I. Boldyrev, and L. S. Wang, J. Chem. Phys. **134**, 224304 (2011).
20. Z. A. Piazza, W.-L. Li, C. Romanescu, A. P. Sergeeva, L. S. Wang, and A. I. Boldyrev, J. Chem. Phys. **136**, 104310 (2012).
21. E. Oger, N. R. M. Crawford, R. Kelting, P. Weis, M. M. Kappes, and R. Ahlrichs, Angew. Chem. Int. Ed. **46**, 8503 (2007).
22. T. B. Tai, N. M. Tam, and M. T. Nguyen, Chem. Phys. Lett. **530**, 71 (2012).
23. D. Y. Zubarev and A. I. Boldyrev, J. Comput. Chem. **28**, 251 (2007).
24. A. Batalov, J. Fulara, I. Shnitko, and J. P. Maier, Chem. Phys. Lett. **404**, 315 (2005).
25. L. Chacaga, E. B. Jochnowitz, Z. Guennoun, H. B. Ding, and J. P. Maier, Int. J. Mass Spectrom. **280**, 174 (2009).
26. L. Cheng, J. Chem. Phys. **136**, 104301 (2012).
27. T. Omi, H. Shitomi, N. Sekiya, K. Takazawa, and M. Fujii, Chem. Phys. Lett. **252**, 287 (1996).
28. H. B. Fu, Y. J. Hu, and E. R. Bernstein, J. Chem. Phys. **124**, 024302 (2006).
29. S. A. Krasnokutski, Y. Lei, J. S. Lee, and D. S. Yang, J. Chem. Phys. **129**, 124309 (2008).
30. A. Fielicke, J. T. Lyon, M. Haertelt, G. Meijer, P. Claes, J. de Haeck, and P. Lievens, J. Chem. Phys. **131**, 171105 (2009).
31. M. Haertelt, J. T. Lyon, P. Claes, J. de Haeck, P. Lievens, and A. Fielicke, J. Chem. Phys. **136**, 064301 (2012).
32. M. Haertelt, A. Fielicke, G. Meijer, K. Kwapien, M. Sierka, and J. Sauer, Phys. Chem. Chem. Phys. **14**, 2849 (2012).
33. See Supplementary Material Document No. _____ for the calculated ionization potentials.
34. A. Fielicke, G. von Helden, and G. Meijer, Eur. Phys. J. D **34**, 83 (2005).
35. A. D. Becke, J. Chem. Phys. **98**, 5648 (1993).
36. S. H. Vosko, L. Wilk, and M. Nusair, Can. J. Phys. **58**, 1200 (1980).
37. C. T. Lee, W. T. Yang, and R. G. Parr, Phys. Rev. B **37**, 785 (1988).
38. L. L. Pan, J. Li, and L. S. Wang, J. Chem. Phys. **129**, 024302 (2008).

39. F. Li, P. Jin, D. Jiang, L. Wang, S. B. Zhang, J. Zhao, and Z. Chen, J. Chem. Phys. **136**, 074302 (2012).
40. C. Adamo and V. Barone, J. Chem. Phys. **110**, 6158 (1999).
41. J. M. Tao, J. P. Perdew, V. N. Staroverov, and G. E. Scuseria, Phys. Rev. Lett. **91**, 146401 (2003).
42. M. S. Gordon, J. S. Binkley, J. A. Pople, W. J. Pietro, and W. J. Hehre, J. Am. Chem. Soc. **104**, 2797 (1982).
43. W. J. Pietro, M. M. Francl, W. J. Hehre, D. J. Defrees, J. A. Pople, and J. S. Binkley, J. Am. Chem. Soc. **104**, 5039 (1982).
44. T. Clark, J. Chandrasekhar, G. W. Spitznagel, and P. V. Schleyer, J. Comput. Chem. **4**, 294 (1983).
45. M. J. Frisch, *et al*. GAUSSIAN 03, Rev. C.02, Gaussian, Inc., Wallingford, CT, 2004.
46. J. S. Binkley, J. A. Pople, and W. J. Hehre, J. Am. Chem. Soc. **102**, 939 (1980).
47. M. P. Andersson and P. Uvdal, J. Phys. Chem. **109**, 2937 (2005).
48. T. B. Tai, D. J. Grant, M. T. Nguyen, and D. A. Dixon, J. Phys. Chem. A **114**, 994 (2010).
49. H. Tang and S. Ismail-Beigi, Phys. Rev. Lett. **99**, 115501 (2007).
50. H. Tang and S. Ismail-Beigi, Phys. Rev. B **82**, 115412 (2010).
51. T. R. Galeev, Q. Chen, J. C. Guo, H. Bai, C. Q. Miao, H. G. Lu, A. P. Sergeeva, S. D. Li, and A. I. Boldyrev, Phys. Chem. Chem. Phys. **13**, 11575 (2011).

Figure captions

Figure 1. Mass spectra of B_n clusters obtained by ionization with an F_2 laser (157 nm, 7.87 eV) using a target made from isotopically-enriched ^{11}B (99.4%). The mass spectra contains carbide and oxide contaminations. The inset shows the detailed assignment for a selected mass range. At the photon energy of 7.87 eV, the ionization efficiency of the pure boron clusters, as well as the contaminations, is strongly size dependent. The lower trace shows the IR induced enhancement for B_{16} and B_{17} at 1100 cm^{-1}.

Figure 2. IR-UV2CI spectrum of B_{11} (top) compared with the IR spectra of low lying isomers from DFT calculation (PBE0/6-311+G(d)). The open circles in the top spectrum correspond to the original data points folded with a 7-point binomial weighted average (solid line). The calculated spectra were generated using Gaussian line widths of 2% of the central wave number.

Figure 3. IR-UV2CI spectrum of B_{16} (top) compared with predicted IR spectra of low lying isomers at the PBE0/6-311+G(d) level of theory. See Fig. 2 caption.

Figure 4. IR-UV2CI spectrum of B_{17} (top) and comparison with the IR spectra of low lying isomers at the PBE0/6-311+G(d) level of theory. See Fig. 2 caption.

Figure 5. The global minima and top three low-lying isomers of B_{11} (A), B_{16} (B), and B_{17} (C). Relative energies in eV are given at the PBE0/6-311+G(d) level, TPSS/6-311+G(d) level (in parenthesis), and B3LYP/6-311+G(d) level (curly brackets). All values are corrected for zero-point vibrational energies, except for structure 17-II at the TPSS/6-311+G(d) level of theory, which is a saddle point (see text).

Figure 1.

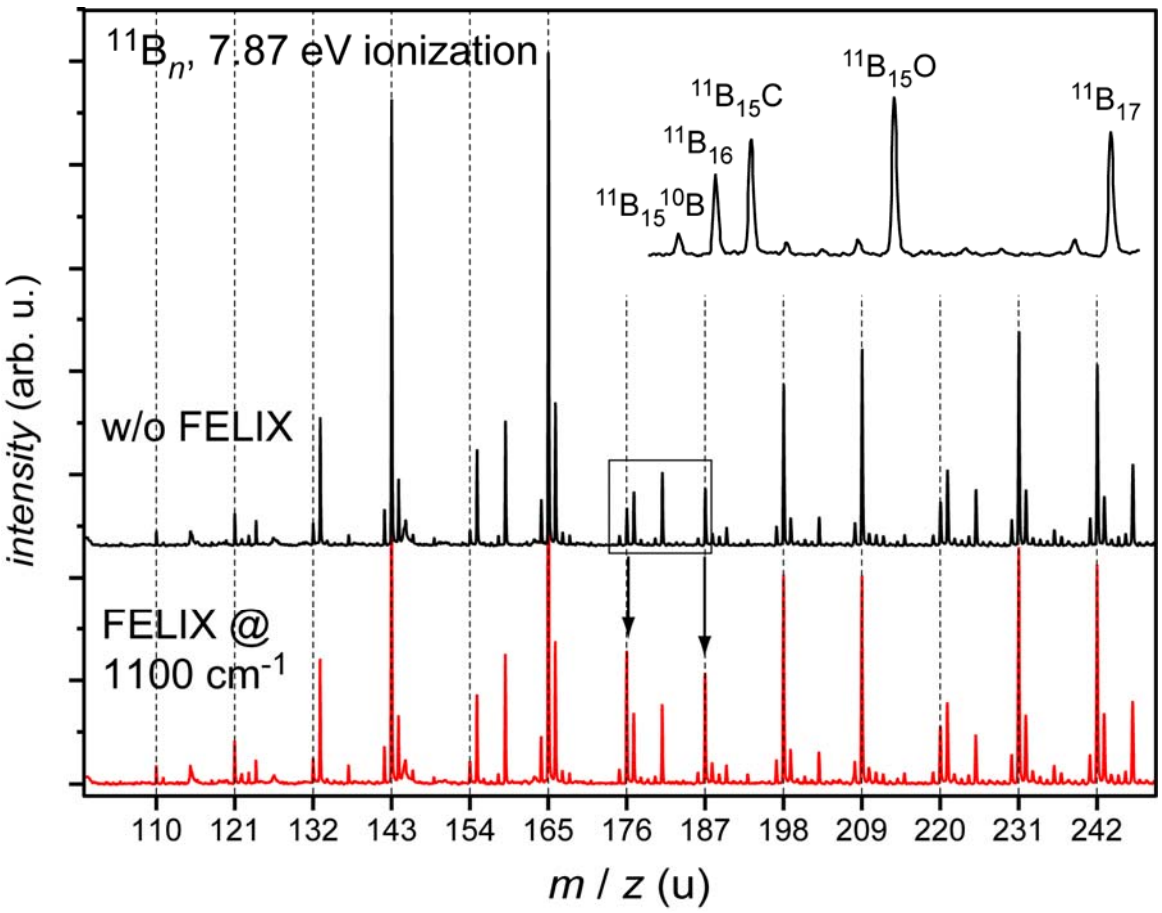
$^{11}B_n$, 7.87 eV ionization
$^{11}B_{15}O$
$^{11}B_{15}C$
$^{11}B_{17}$
$^{11}B_{16}$
$^{11}B_{15}{}^{10}B$
w/o FELIX
FELIX @
1100 cm^{-1}
intensity (arb. u.)
110 121 132 143 154 165 176 187 198 209 220 231 242
m / z (u)

Figure 2

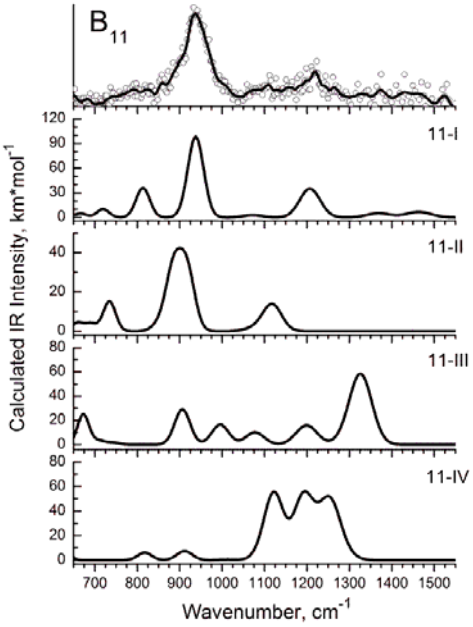
B11
11-I
11-II
11-III
11-IV
Calculated IR Intensity, km*mol-1
Wavenumber, cm-1

Figure 3.

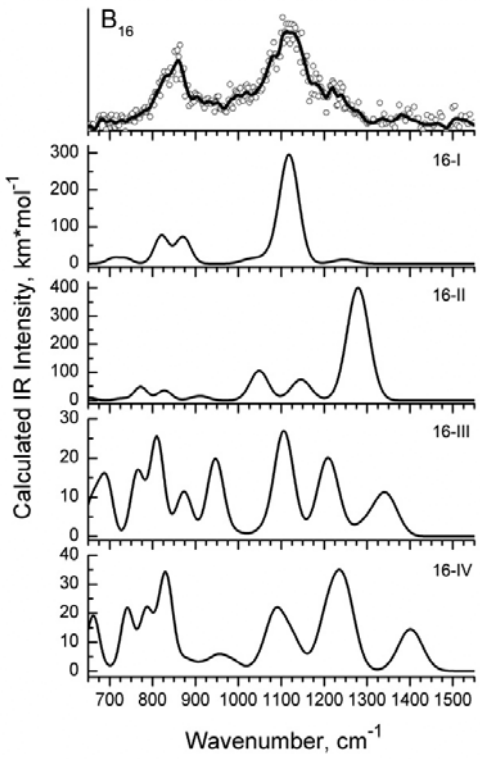
B16
16-I
16-II
16-III
16-IV
Calculated IR Intensity, km*mol-1
Wavenumber, cm-1
700 800 900 1000 1100 1200 1300 1400 1500

Figure 4.

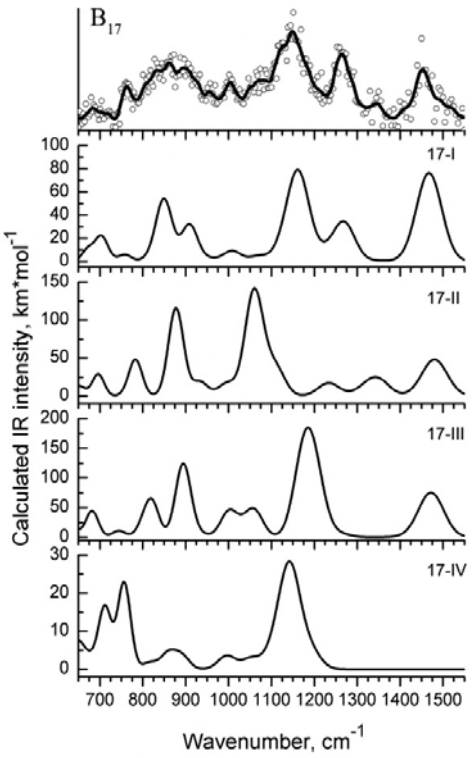
B17
17-I
17-II
17-III
17-IV
Calculated IR intensity, km*mol-1
Wavenumber, cm-1
700 800 900 1000 1100 1200 1300 1400 1500

Figure 5.

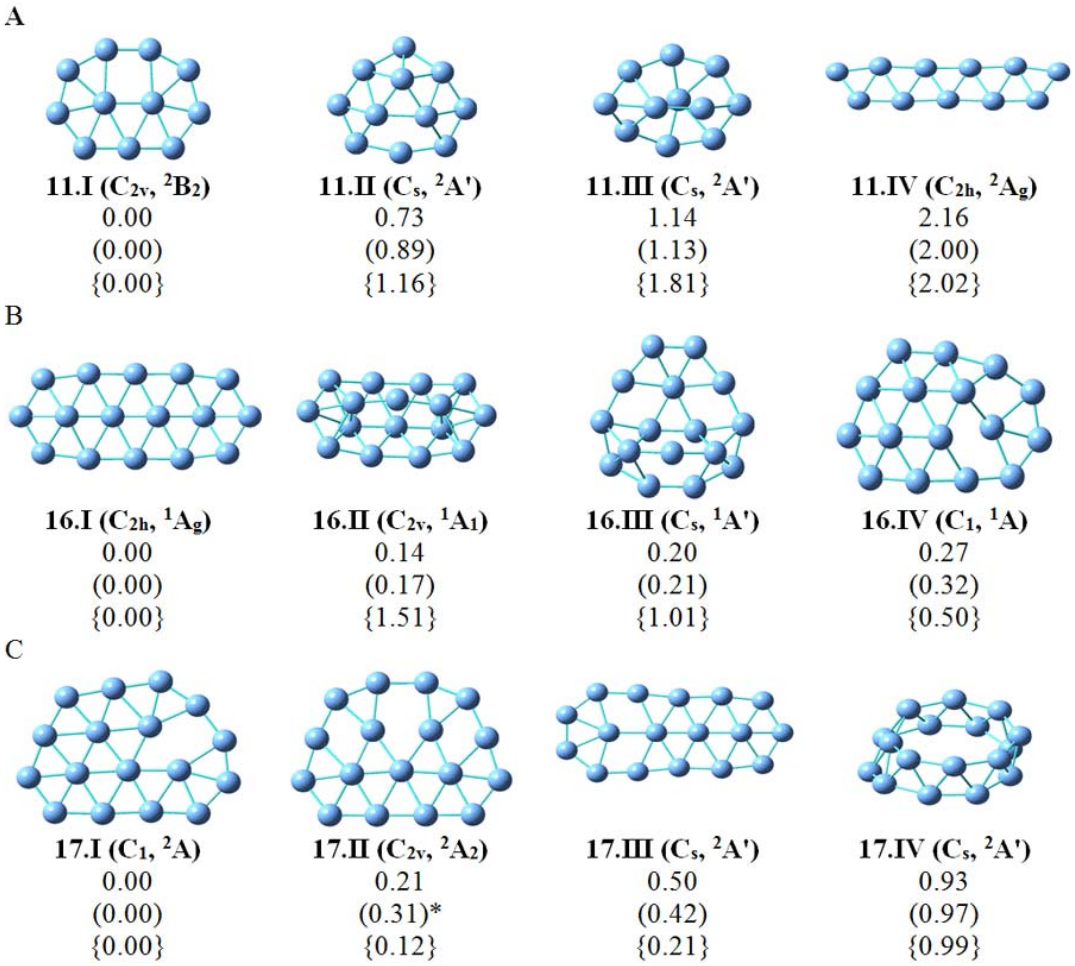
A
11.I (C_{2v}, $^2B_2$)
0.00
(0.00)
{0.00}
11.II (C_s, $^2A'$)
0.73
(0.89)
{1.16}
11.III (C_s, $^2A'$)
1.14
(1.13)
{1.81}
11.IV (C_{2h}, ^2A_g)
2.16
(2.00)
{2.02}
B
16.I (C_{2h}, ^1A_g)
0.00
(0.00)
{0.00}
16.II (C_{2v}, $^1A_1$)
0.14
(0.17)
{1.51}
16.III (C_s, $^1A'$)
0.20
(0.21)
{1.01}
16.IV (C_1, ^1A)
0.27
(0.32)
{0.50}
C
17.I (C_1, ^2A)
0.00
(0.00)
{0.00}
17.II (C_{2v}, $^2A_2$)
0.21
(0.31)*
{0.12}
17.III (C_s, $^2A'$)
0.50
(0.42)
{0.21}
17.IV (C_s, $^2A'$)
0.93
(0.97)
{0.99}